

Development of Sustainable Nanocomposites from Cellulose Ester For Automotive Applications

Hwan-Man Park¹, Amar K. Mohanty², Manjusri Misra¹ and Lawrence T. Drzal¹

¹Composite Materials and Structures Center, 2100 Engineering Building,
Michigan State University, East Lansing, MI-48824,

²The School of Packaging, 130 Packaging Building,
Michigan State University, East Lansing, MI 48824,

Abstract

Sustainable nanocomposites have been successfully fabricated from renewable cellulose acetate (CA), environmentally benign triethyl citrate (TEC) plasticizer and organically modified clay. The effects of processing conditions, such as mixing methods, pre-plasticizing times, retention times (RT), and addition of compatibilizer maleic anhydride grafted cellulose acetate butyrate (CAB-g-MA) on the performance of these nanocomposites, have been evaluated. The cellulosic plastic with CA/TEC (80/20 or 75/25 wt. %) was used as the polymer matrix for nanocomposite fabrication. The morphologies of these nanocomposites were evaluated through X-ray diffraction (XRD), Atomic force microscope (AFM), and transmission electron microscopy (TEM) studies. From all the sequential mixing methods used, powder-powder mixing leads to the most transparent nanocomposites. Cellulosic plastic-based nanocomposites obtained using increased pre-plasticizing times and RT showed better-exfoliated structures. Cellulosic plastic-based nanocomposites with 5 wt.% compatibilizer contents showed better-exfoliated structure than the counterpart having 0 or 7.5 wt.% compatibilizer contents. Polygonal shape of exfoliated clay platelets was observed with 500 nm width, and 800 nm length by AFM and TEM imaging. The mechanical properties of the nanocomposites have been correlated with the XRD and TEM observations.

Introduction

Nanocomposites offer the potential for the diversification and application of polymers due to their excellent properties such as high heat distortion temperature, dimensional stability, improved barrier properties, flame retardancy, and enhanced physico/thermo-mechanical properties. Polymer layered silicate nanocomposites have been studied for nearly 50 years [1], although the concept was first introduced by researchers from Toyota [2] who made nanocomposites from polyamide 6 and organophilic clay. An extensive literature is now available on nanocomposites with matrices of epoxy [3, 4], polyamide, polystyrene, polyurethane, poly (ethylene terephthate) and polypropylene. Automakers see application opportunities for polymer clay nanocomposites especially with polypropylene (PP), thermoplastic polyolefin (TPO) and nylon-based nanocomposites [5]. Renewable resource-based biodegradable polymers including cellulosic plastic (plastic made from wood), polylactic acid, PLA (corn-derived plastic) and polyhydroxyalkanoate, PHA (bacterial polyesters) are some of the potential biopolymers which with effective reinforcement with nanoclay can become so called 'green' nanocomposites [6].

Cellulose from trees is attracting interest as a substitute for petroleum feedstock in making plastic (cellulosic plastic - cellulose esters) in the commercial market [7]. Cellulosic plastics like cellulose acetate (CA), cellulose acetate propionate (CAP), and cellulose acetate

butyrate (CAB) are thermoplastic materials produced through esterification of cellulose. The main drawback of cellulose acetate plastic is that its melt processing temperature exceeds its decomposition temperature and to overcome this drawback, it should be plasticized. The phthalate plasticizer, used in commercial cellulose ester plastic, is now under environmental scrutiny and perhaps poses a health threat and thus there is some concern about its long-term use. One of our main purposes is to replace phthalate plasticizer by an eco-friendly plasticizer like citrate [8, 9] and blends of citrate and derivitized vegetable oil in designing more eco-friendly cellulosic plastic formulations.

In our current investigations on cellulose acetate plastic-clay based nanocomposites we have chosen triethyl citrate as the plasticizer. Melt processing through extrusion-injection molding is adopted in fabricating the nanocomposites. By adding organically modified montmorillonite clays into plasticized CA matrix during melt extrusion with high shear force, exfoliated and/or intercalated clay is expected to be produced inside the continuous matrix. Pre-plasticization time is defined as the time required for the plasticizer to be imbibed by the CA plastic, to yield a free-flowing powder that will feed properly into extruders [10]. Pre-plasticizing times, optimized processing conditions and sequential mixing methods, and compatibilizer CAB-g-MA are investigated in this paper. Morphological (X-ray diffraction (XRD), Transmission Electron Microscope (TEM)) and mechanical and thermal properties were evaluated.

Experimental Details

Materials: Cellulose acetate, CA (CA-398-30) without additives in powder form and triethyl citrate (TEC, Citroflex 2) were supplied by Eastman Chemicals Co., Kingsport, TN and Morflex, Inc. North Carolina, respectively. The degree of substitution of cellulose acetate (CA) is 2.5. One kind of organically modified montmorillonite (organoclay Cloisite 30B) was purchased from Southern Clay Co., Texas. The ammonium cation of Cloisite 30B is methyl tallow bis-2-hydroxyethyl quaternary ammonium. The compatibilizer, CAB-g-MA, was synthesized by radical graft polymerization of MA monomer onto the CAB backbone polymer and characterized as reported by us earlier [11]. The calculated acid number and grafting percentage (MA wt.-%) were 18.6 and 0.86 wt.-%, respectively.

Melt compounding: The CA and clay were dried under vacuum at 80 °C for at least 24 hrs before use. The CA powder and TEC plasticizer (CA:TEC = 80:20 by wt. %) were mixed mechanically with a high speed mixer for about 5 min and CA pre-plasticized mixture was stored in zip-lock bags for 20, 40 and 75 minutes. These pre-plasticized mixtures were then mixed with 5 wt. % of organoclays followed by mixing in the high speed mixer. Then such mixtures (CA + TEC + Organoclay + compatibilizer) were melt compounded at 220°C for 6 minute at 100 rpm in micro-compounding molding equipment, DSM Micro 15 cc mini extruder with injection molder (DSM research, Netherlands).

Characterization of nanocomposite: XRD studies of the samples were carried out using a Rigaku 200B X-ray diffractometer (45 kV, 100 mA) equipped with CuK α radiation ($\lambda= 0.1516$ nm) and a curved graphite crystal monochromator at a scanning rate of 0.5 °/min. A transmission electron microscope (TEM) (Jeol 100CX) was used to analyze the morphology of nanocomposites at an acceleration voltage of 100 kV. Microtomed ultra thin film specimen with thickness of ~70 nm was used for TEM observation. Microscope photography used Olympus BH-2 (Japan). A dynamic mechanical analyzer (2980 DMA, TA instruments, USA) was used to measure the dynamic storage modulus (E'), loss modulus (E'') and mechanical loss tangent (tan

$\delta = E''/E'$). Flexural properties of injection mold specimens were measured with a United Testing System SFM-20 according to ASTM D790. AFM characterization was conducted using a Nanoscope IV atomic force microscope from Digital Instruments (Santa Barbara, CA) equipped with an E scanner. Samples were mounted onto a stainless steel disk using a sticky tab (Latham, NY). The microscope was allowed to thermally equilibrate for thirty minutes before imaging. Scanning rates less than 1 Hz were used. Room temperature was maintained at 22 ± 1 °C. Images were recorded in tapping mode using etched silicon probes (Digital Instruments).

Results and Discussion

Sequential Mixing Methods: Figure 1 shows the micrographs of different sequential mixing methods for CA powder, clay, and non-solvent type plasticizer TEC for homogeneous clay dispersion hybrid nanocomposites. Figure 1a shows plasticized CA/TEC pellets mixed with clay and then melt compounded. Figure 1b shows the results of addition of clay powder while melting the CA/TEC powder, followed by continued melt compounding in the extruder. These two conventional methods result in non-transparent composites due to aggregated or poorly dispersed clay in the matrix (see Figure 1a and 1b). Figure 1c shows the TEM image of our developed powder-powder mixing method, i.e., powdered form of cellulose acetate was pre-plasticized by the addition of TEC, then clay powder mixing, followed by melt compounding in extruder. Such a hybrid powder-powder mixing method produced the best dispersion of clay which resulted in homogeneous dispersion and exfoliation.

Figure 2 show DSC curves of CA raw material and CA/TEC/clay hybrid. CA raw material is a semi-crystalline polymer which has a melting temperature (T_m) of 211 °C and glass transition temperature (T_g) of 175 °C in the first heating curve (Figure 2a), but in second heating (figure 2a) the T_m peak is absent and only the T_g 175°C peak is present. Also the plasticized CA hybrid (Figure 2b) shows only a T_g peak at 177 °C. This means that that the CA structure

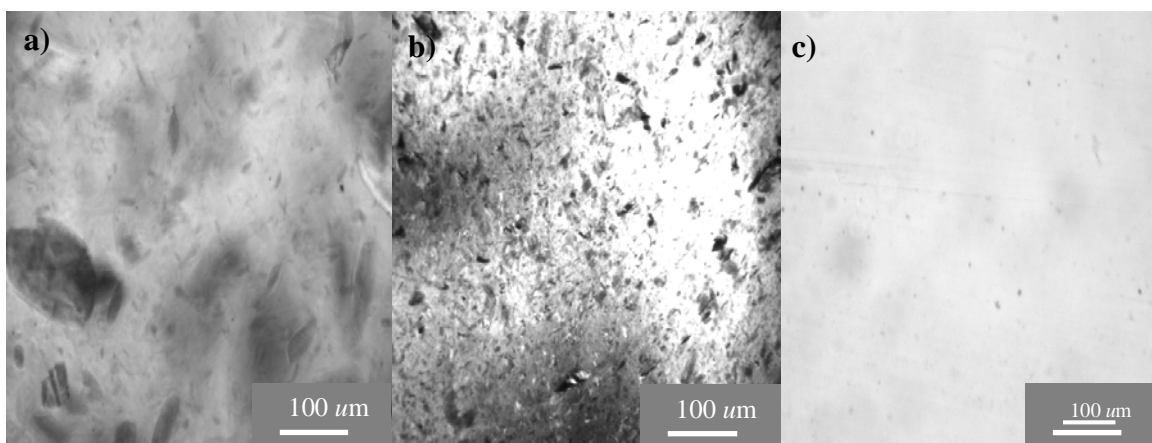


Figure 1. Micrographs of the CA/TEC/clay hybrid nanocomposites with different sequential methods: a) CA/TEC plasticized pellet + clay mixing, b) CA/TEC melting + clay mixing, c) pre-plasticized CA/TEC powder + clay mixing; Olympus BH-2 (Japan)-80X .

became amorphous due to difficulty in re-crystallization. R. E. Boy et al. reported similar DSC behavior of CA [12].

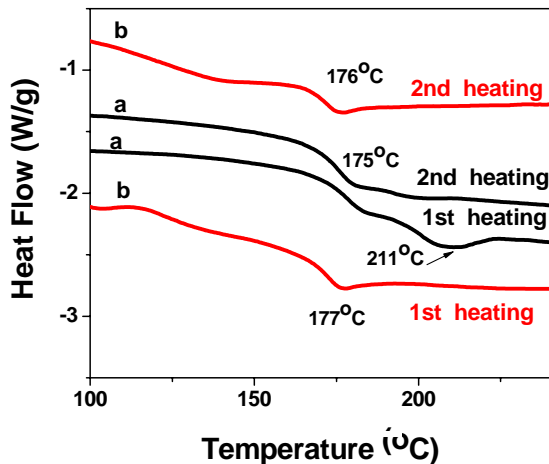


Figure 2. DSC curves of the CA/TEC/clay hybrid nanocomposites and CA raw material: a) CA powder raw, b) CA/TEC/clay hybrid.

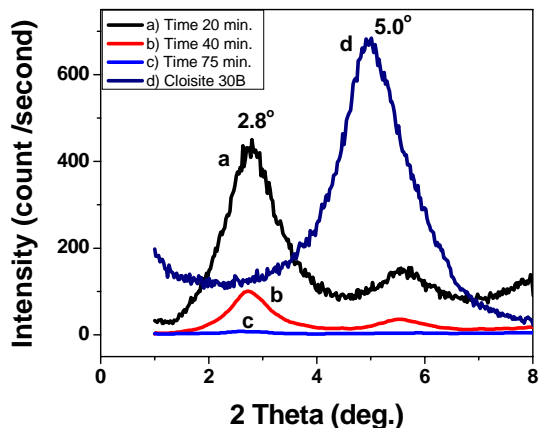


Figure 3. XRD patterns of the CA/TEC/clay hybrid nanocomposites with different pre-plasticizing times: a) 20min, b) 40 min c) 75 min, d) Cloisite 30B.

In pre-plasticization study, the penetration time of TEC plasticizer into CA powder and the melt compounding are very important parameters for plasticizing CA/TEC plastic. In [Table 1](#) the effect of sequential mixing method and pre-plasticizing time on flexural properties of these hybrid nanocomposites is shown. The powder-powder mixing hybrid process produces good flexural strength and modulus. This mixing method is used to prepare the following powder-powder systems.

Microstructure of nanocomposites: [Figure 3](#) shows the XRD patterns of pure Cloisite 30B clay and CA/TEC/ Cloisite 30B nanocomposites with different pre- plasticizing times. The XRD peak shifted from $2\theta=5.0^\circ$ for pure Cloisite 30B to 2.8° for 20 minute and 40 minute pre-plasticized CA/TEC Cloisite 30B nanocomposite ([Figure 3a](#) and [3b](#)). This indicates significant intercalation and slight exfoliation in the hybrid structure. For CA/TEC/Cloisite 30B nanocomposite after 75 minute pre- plasticizing times ([Figure 3c](#)), no clear peak was observed at 2.8° , suggesting complete exfoliation of organoclays in the CA/TEC matrix.

In [Figure 4](#), the TEM images show that the 75 minute pre- plasticizing time CA/TEC/Cloisite 30B hybrid produces the best exfoliation. It can also be seen that the intercalation of clay decreases with increase in pre- plasticizing times. In the TEM and XRD curves, about 75 minute of penetration time is required for almost completely exfoliated clay nanocomposites for the CA/TEC/clay system.

Mechanical Properties: [Table 1](#) show typical flexural properties of the CA/TEC/Cloisite 30B hybrids with different pre-plasticizer times. The flexural strength and modulus of the CA/TEC/organoclay hybrids increased with increasing pre-plasticizing time. An optimal penetration time is need for the nonsolvent plasticizer TEC to migrate into and in between the

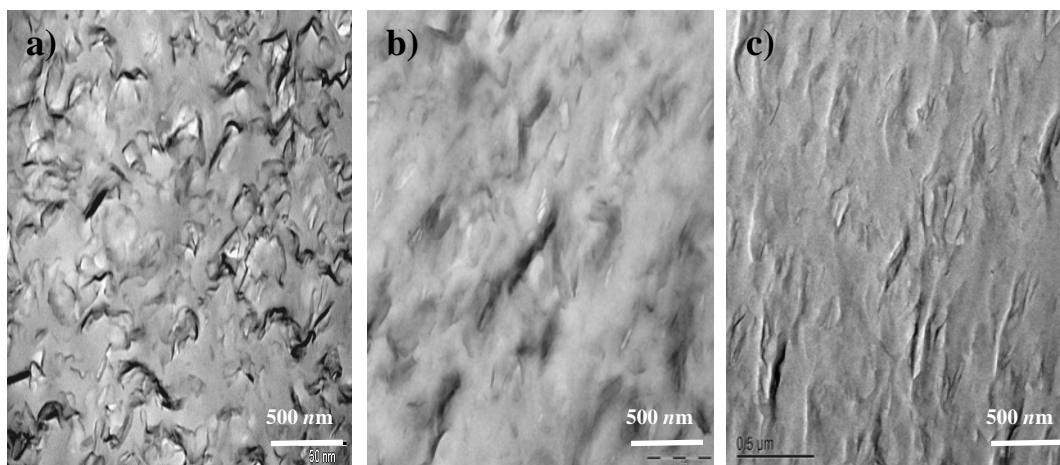


Figure 4. TEM micrographs of the CA/TEC/organoclay hybrid nanocomposites obtained from CA/TEC (80/20 wt.-%) and organoclay 5 wt.-%, by compounding at 200°C, using a retention time of 10 minutes and different pre-plasticizing times: a) 20 min, b) 40 min, c) 75min.

Table 1 Flexural properties of the CA/TEC/clay hybrid nanocomposites with different sequential mixing methods and pre-plasticizing times.

| Sample No | Sequential mixing method | Pre-plasticizing time (min.) | Clay content (wt%) | Flexural Strength (MPa) | Flexural Modulus (GPa) |
|-----------|---|------------------------------|--------------------|-------------------------|------------------------|
| 1 | CA/TEC plasticized pellet + clay powder | 75 | 5 | 94 ± 2.2 | 4.00 ± 0.1 |
| 2 | CA/TEC melting + clay powder | 75 | 5 | 93 ± 0.7 | 4.08 ± 0.1 |
| 3 | CA/TEC pre-plasticized powder + clay powder | 75 | 0 | 84 ± 4.4 | 3.00 ± 0.3 |
| 4 | | 20 | 5 | 93 ± 3.0 | 3.75 ± 0.4 |
| 5 | | 40 | 5 | 95 ± 2.1 | 3.89 ± 0.6 |
| 6 | | 75 | 5 | 98 ± 3.0 | 4.10 ± 0.5 |

rigid CA molecular chain making CA plastic flexible and soft. The above results indicate that the better exfoliation and good dispersion of clay in the CA/TEC matrix gives good mechanical properties.

Dynamic Mechanical Properties: Figure 5 shows temperature dependent storage modulus, $\tan \delta$, and glass transition temperature (T_g) respectively for the pristine CA/TEC and the nanocomposites for 75 min. pre-plasticized time. Storage modulus & T_g of CA/TEC/clay hybrid composites increased with addition of 5 wt. % clay. The storage modulus of these hybrid composites (5.1 GPa) also increased by 21% as compared to pure CA/TEC matrix (4.20 GPa) at temperature of 30°C. A possible explanation for improvement of modulus with reinforcement of clay might be attributed to the creation of a three-dimensional network interconnecting long silicate layers, thereby strengthening the material through mechanical percolation [13].

On the other hand, the shift and broadening of $\tan \delta$ peak to higher temperatures indicates an increase in T_g and broadening of the glass transition temperature of the nanocomposites with clay content (see Figure 5). The shift in T_g from the $\tan \delta$ peak was 6 °C for the hybrids containing 5 wt. % clay ($T_g = 136^\circ\text{C}$) in contrast to CA/TEC plastic ($T_g = 130^\circ\text{C}$). The broadening and increase of T_g of hybrids after adding Cloisite 30B may be due to the fact that clays create restricted segmental motions near the organic-inorganic interface of the parent cellulosic plastic [13].

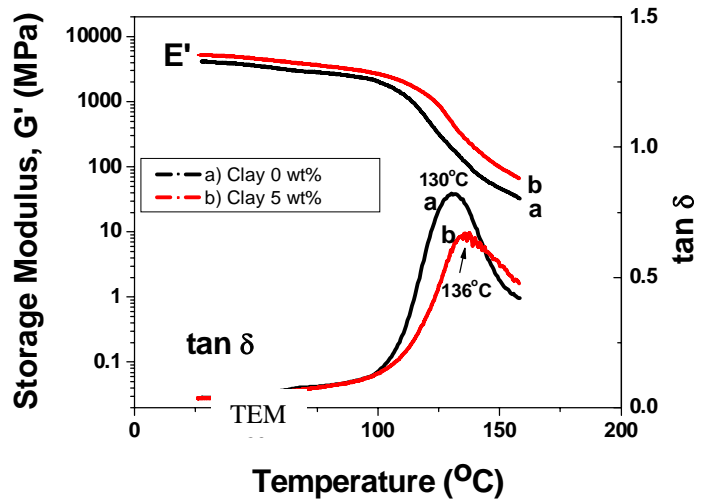


Figure 5. DMA curves of the CA/TEC/clay hybrid nanocomposites at 75 min fixed pre-plasticizing time: a) Cloisite 30B 0 wt%, b) Cloisite 30B 5 wt%.

Effect of the Compatibilizer CAB-g-MA: In order to obtain the better exfoliated nanocomposites, the synthesized compatibilizer was added to the pre-plasticized CA /Cloisite 30B composition at 0, 5, and 7.5 wt.-% content. The 5 wt.-% compatibilizer CAB-g-MA (grafting percentage (MA wt.-%) were 0.86 wt.-%) hybrid nanocomposite show the best morphology and mechanical properties. Therefore, nanocomposites with 5 wt.-% compatibilizer or without compatibilizer were used to investigate the nanostructure.

Figure 6 shows AFM height images of the nanocomposites without compatibilizer (Figure 6a) and with 5 wt.-% compatibilizer (Figure 6b), respectively. An advantage of AFM imaging is the relatively high phase contrast between the soft matrix and the hard silicate particles of the nanocomposites [14]. The images show that the plasticized CA/organoclay/compatibilizer hybrid has better exfoliation nanocomposites than the counterparts without compatibilizer. The intercalated structure of clay is dominant in Figure 6a as labeled by the arrows. Partially

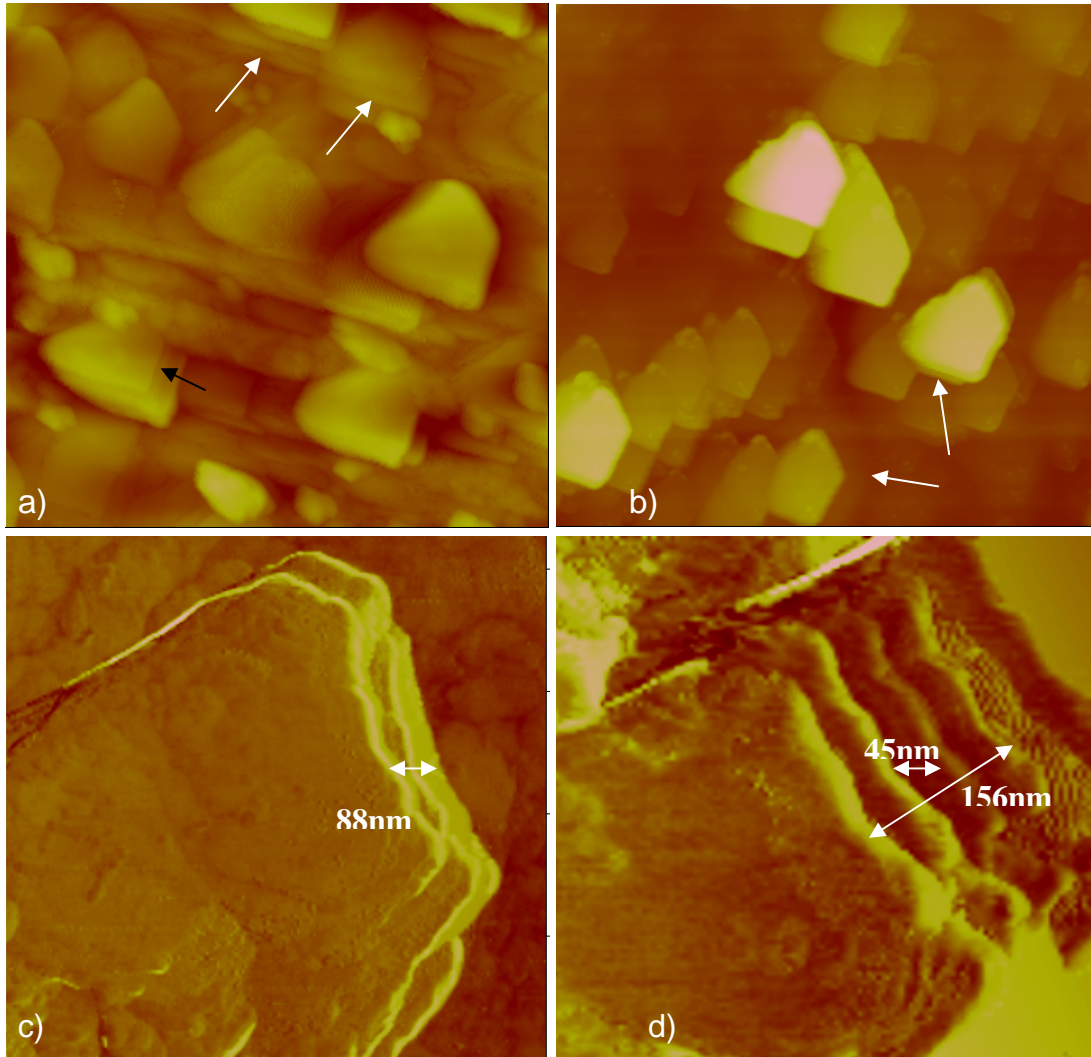


Figure 6. AFM height and phase images of plasticized CA/compatibilizer/organoclay system: a) Plane-sectioned height topographical view of nanocomposite without compatibilizer, scan size 5 μ m; b) Plane-sectioned height topographical view of nanocomposite with compatibilizer 5 wt.-%, scan size 5 μ m; c) Cross-sectioned phase image of intercalate clay without compatibilizer, scan size 0.85 μ m; d) Cross-sectioned phase image of intercalate clay with compatibilizer 5 wt.-%, scan size 0.5 μ m.

exfoliated clay can be seen clearly in Figure 6b (showed by arrows), coexisting with the intercalated clay particles. The width of the clay nanoplatelets is around 500 nm, and the length is around 800 nm. It is obvious that the pentagon shaped clay platelets have been oriented along one direction. This is due to the external force applied to the nanocomposite samples in

the injection molding process. This ordered exfoliated morphology influenced the mechanical and barrier properties of nanocomposites.

Figure 6c and 6d show the cross-section AFM phase images of the intercalated CA/organoclay without and with 5 wt.-% compatibilizer, respectively. Well-defined intercalated clay platelet structure was observed. However, large separations (Figure 6d, each dark strand thickness is 30-45 nm, total distance is about 156 nm) between intercalated clay platelets were observed for the nanocomposite with 5.0 wt.-% compatibilizer compared to that without compatibilizer (Figure 6c).

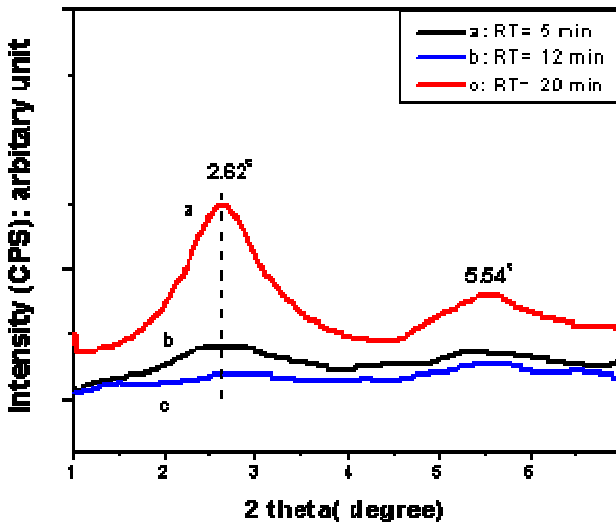


Figure 7. XRD patterns of the plasticized CA / TEC (80/20wt%) organoclay 5 wt% hybrids with different melt compounding RT: a) RT 5 min, b) RT 12 min, c) RT 20 min. pre-plasticizing : 75 minutes, melt compounding temp. 220°C.

Effect of compounding RT: Figure 7 shows XRD patterns of nanocomposites obtained using different compounding retention times (RT) at a fixed melt compounding temperature of 220°C (which is the optimum temperature for the TEC 20 wt % hybrid system). In Figure 7, the intensity of intercalation peak (at $2\theta=2.62^\circ$) decreases with increasing RT. Such increased RT assists in producing a more exfoliated morphology. For retention times higher than 20 minutes, thermal degradation exceeds the effect of improved exfoliation of the organoclay in the hybrid.

Conclusions

Injection molded biodegradable green nanocomposite formulations have been developed from cellulose acetate powder, triethyl citrate plasticizer and organically modified clay. Since, cellulose acetate is biodegradable, the nanocomposite from cellulose acetate, triethyl citrate (TEC) and organoclay is expected to be biodegradable. The powder-powder hybrid mixing method produced the best dispersion of clay and transparent nanocomposites. Among all the different pre-plasticizing times investigated, the 75-minute pre-plasticized hybrid showed the best exfoliation and intercalated state of clay and properties of the resulting nanocomposites. Polygonal shape of exfoliated clay platelets was observed with 500 nm width and 800 nm length by AFM and TEM imaging.

As a result of this research, it has been found that CA nanocomposites show superior flexural strength and modulus (98 MPa and 4.1 GPA) compared to PP nanocomposites (38 MPa, 1.4 GPA).

The cellulose ester used in this current research is obtained in a powder form and costs ~\$1 per pound where as the PP/TPO that are currently used in automotive for

making nanocomposites cost ~\$0.50 - \$1.20 per pound. Considering the cost of clay and processing as constant for both kinds of nanocomposites; the cellulosic plastic-clay nanocomposites has potential for competing with polypropylene-clay nanocomposites for future 'green' automotive parts. Further research is in progress to explore these potential nanocomposites for automotive applications and other high volume uses.

Acknowledgements

Authors are thankful NSF-NER 2002 Award # 0210681, NSF 2002 Award # DMR-0216865 for financial support. The collaboration with FORD MOTOR COMPANY and EASTMAN CHEMICAL Co. is gratefully acknowledged.

References

1. Carter, L. W., Hendricks, J. G. and Bolley, D. S., U. S. Pat. 2,531,396, (1950).
2. Okada, O., Kawasumi, M., Usuki, A., Kurauchi, T. and Kamigaito, O., Mater Res Soc Symp Proc 171, 45 (1990).
3. Pinnavaia, T. J., Lan, T., Wang, Z., Shi, H. and Kavaratna, P. D., ACS Symp Ser 622, 250 (1996).
4. Messersmith, P. B. and Giannelis, E. P., Chem Mater, 6, 1719 (1994).
5. Mohanty, A. K., Misra, M. and Drzal, L. T., Proceedings of 9th Annual Global Plastics Environmental Conference (GPEC 2002),
6. Mohanty, A. K., Drzal, L. T. and Misra, M., Polymeric Materials Science & Engineering, 88, 60-61 (2003).
7. Wilkinson, S. L., Chem. Eng. News, January 22, 61 (2001).
8. Mohanty, A. K., Wibowo, A., Misra, M. and Drzal, L. T., Polymer Engineering & Science, 43: 5, 1151-1161 (2003).
9. Park, H.-M., Mohanty, A. K., Misra, M. and Drzal, L. T., Biomacromolecular, Accepted and in press (July 2004).
10. Bruins, P. F., In *Plastic Technology*; New York Reinhold Publishing Co. Chapman & Hall, Ltd., London, 1, 1-7, 193-199, (1965).
11. Wibowo, A.; Mohanty, A. K.; Misra, M.; Drzal, L. T. *Polymer Preprint*, Spring 2004, 45(1), 1058, 227th ACS Spring National Meeting, Anaheim, CA, (2004).
12. Boy, R. E. and Schulken, R. M., J. Appl. Polym. Sci., 11, 2453-2465, (1967).
13. Giannelis, E.P. and Messersmith, P.B., US Patent 5554670, Sep. 10, (1996).
14. Bar, G., Thomann, Y., Brandsch, R., Cantow, H.-J. and Whangbo, M. H. Langmuir, 13, 3807, (1997).

Keywords: cellulose acetate, compatibilizer, nanocomposites, organoclay, extrusion